Structure of the effective Hamiltonian for liquid-vapor interfaces

M. Napiórkowski
Instytut Fizyki Teoretycznej, Uniwersytet Warszawski, Hoża 69, 00-681, Warszawa, Poland

S. Dietrich
Fachbereich Physik, Bergische Universität Wuppertal, Postfach 100127, D-5600 Wuppertal 1, Germany
(Received 24 September 1992)

Using the microscopic density-functional theory for inhomogeneous simple fluids, we derive a nonlocal and non-Gaussian expression for the effective Hamiltonian of a fluctuating liquid-vapor interface. If a gradient expansion is applied to this Hamiltonian, one obtains—after a partial resummation—as the leading term the standard effective interface Hamiltonian which is proportional to the increase of the area of the interface relative to that of the flat configuration. The next to leading terms are proportional to the Gaussian and to the mean curvature of the interface, respectively. Microscopic expressions for the coefficients in this expansion are derived. If the interparticle interactions in the fluid decay according to power laws, the gradient expansion breaks down. This is reflected in the nonanalytic behavior of the wave-vector-dependent surface tension which can be expressed in terms of the Fourier transform of the interaction potential between the fluid particles. Various approximations of the nonlocal Hamiltonian are compared quantitatively. The relevance of this Hamiltonian for interpreting scattering experiments is discussed.

PACS number(s): 68.10.Cr, 68.15.+e, 61.25.Bi

I. INTRODUCTION

The understanding of the structure of fluid interfaces poses an outstanding challenge for both theoretical and experimental physics [1–5]. This interest has been increased even further by the discovery of interfacial phase transitions such as wetting, surface melting, layering, etc., because these phenomena result from the interaction between emerging interfaces where at least one of them is a fluid-fluid interface. Therefore its structure determines *inter alia* the corresponding thermodynamic singularities of such interfacial phase transitions.

In spite of numerous contributions to this field its complexity has so far prevented a satisfactory and complete understanding of the structural properties of fluid interfaces. The present knowledge is based on various approximations which focus on different aspects of the problem and which are sometimes incompatible with each other. Naturally this situation has led to numerous discussions in the literature, many of them being stimulated by the seminal paper by Buff, Lovett, and Stillinger [6].

One way of approach to the description of an interface separating two fluid phases follows the ideas formulated initially by van der Waals [7]. Within this approach the existence of an interface is an *intrinsic* property of an inhomogeneous fluid where two phases coexist (they are separated by appropriate boundary conditions). In particular, the existence of the interface does not require such external agents as gravity, the finite size of the system, or a substrate with which the interface interacts. Accordingly, within this approach, the density profile present in an inhomogeneous system exhibiting an interface is called the intrinsic density profile $\rho_{\mathrm{int}}(z)$. In a second step this flat intrinsic interface is used as the starting point for a more complete description of the actual interface. It may be seen as a "skeleton" on which ripples—traditionally called capillary waves—are unfrozen. These ripples are considered to be an inherent part of the actual interfacial structure though they are not included in the concept of the intrinsic density profile. Along this line of reasoning the full interfacial structure is determined with the help of the effective interface Hamiltonian. So far this Hamiltonian [8–12] has been constructed phenomenologically in such a way as to include the cost in free energy to deform the initially flat interface into a given rippled configuration. In the third step the effective interface Hamiltonian is used in the Boltzmann factor with which different configurations of the deformed interface are weighted.

Although attractive in its conceptual construction the van der Waals approach lacks a rigorous basis and misses the fact that without gravity and in spatial dimensions $d \leq 3$ the fluid interface is rough. An important conceptual improvement was achieved by Weeks [13] and Bedeaux and Weeks [14] who argued that the density fluctuations with wavelengths up to the bulk correlation length ξ contribute to the intrinsic density profile while the fluctuations with wavelengths larger than ξ are represented by the capillary waves unfrozen as undulations on this intrinsic profile. This picture was supported by model calculations [13] but a rigorous microscopic justification is still missing. Such a microscopic approach should open the possibility of identifying both the intrinsic and capillary wave contributions to the interfacial structure together with a clear definition of the range of the wavelengths of the density fluctuations corresponding to the two regimes mentioned above. Equally important, such an approach should also produce the expression for

the effective interface Hamiltonian. So far most of the attempts to derive the effective interface Hamiltonian are based on the coarse-grained standard Landau theory or modifications thereof [15–18]. After tracing out all degrees of freedom but the local interface position, one obtained the corresponding effective Hamiltonian which—within this approach—is, as phenomenologically expected, the sum of the geometrical invariants of the interface: the area of the interface, its mean curvature and the square of it, and the Gaussian curvature. The corresponding coefficients of these terms turn out to be moments of the square of the derivative of the intrinsic interface profile. Recently, this Landau-type approach has been extended [19] in order to derive the Helfrich Hamiltonian [20,21]. These authors determine the coefficients corresponding to the geometrical invariants entering the effective interface Hamiltonian by evaluating the Landau free energy for two particular interface configurations: a sphere and a cylinder.

Although it is pleasing to see that the phenomenological form of the effective interface Hamiltonian can be deduced from a more complete bulk theory, the Landau theory does not allow one to keep track of the microscopic details of the fluid. First steps have been undertaken in order to overcome these shortcomings by resorting to an expansion of the free energy density in powers of curvatures for spheres and cylinders [22], to a gradient expansion [23–25] or to an expansion in powers of the range of the intermolecular interaction potential [26]. These approaches lead again to the phenomenological form of the effective interface Hamiltonian but such that its corresponding coefficients are now expressed in terms of microscopically defined distribution functions of the nonuniform fluid.

In this paper we adopt a still different approach by using the density-functional theory [27,28] as a starting point, which has proven to be particularly successful in describing nonuniform fluids on a microscopic level. This allows us to determine the effective interface Hamiltonian without using the gradient expansion which is inherent in the other microscopic models [29–31]. This more general approach leads to a *nonlocal* and *nonbilinear* effective interface Hamiltonian which *differs* from those which have been obtained previously. Some results of this approach can be found in Refs. [32,33]. For smooth interface configurations our Hamiltonian reduces to the standard phenomenological form provided that the pair interaction potential between the fluid particles fulfills certain conditions. It turns out that for realistic fluids with van der Waals interactions the nonlocal Hamiltonian cannot be replaced by the standard phenomenological one. We compare the various approximations quantitatively and discuss the implications of our findings for the interpretation of data gathered from scattering experiments at interfaces.

II. THE MODEL

In order to derive the effective interface Hamiltonian we employ a simple version of the density-functional theory. In this approach the nonuniform equilibrium density profile minimizes the appropriate variational functional. This functional depends parametrically on the thermodynamic state of the system and on the microscopic interactions present in the system, i.e., on the particle-particle interaction potential $w(\mathbf{r})$ as well as on the external field $V(\mathbf{r})$. The density functional evaluated at the equilibrium density profile is equal to the appropriate thermodynamic potential.

In the following we use the grand canonical density functional $\Omega(\{\rho(\mathbf{r})\},T,\mu;\{w(\mathbf{r})\},\{V(\mathbf{r})\})$ in which the thermodynamic state is specified by the temperature T and the chemical potential μ. We consider only one-component fluids with spherically symmetric interaction potentials. In its general formulation the knowledge of the explicit form of the density functional allows one—in principle—not only to determine the density of the system but also the whole hierarchy of correlation functions. However, in practice one is forced to work with approximate forms of the density functionals. This reflects our still incomplete knowledge about the properties of nonuniform fluid systems.

The approximation used in this paper is, as for all known explicit density functionals, mean-fieldlike. It is based on splitting the potential $w(\mathbf{r})$ between the fluid particles into its short-range repulsive part $w_h(\mathbf{r})$ and into its long-range attractive part $w_l(\mathbf{r})$ [34]:

$$w(r)=w_h(r)+w_l(r)\ . \tag{2.1}$$

This splitting is reflected in the contributions to the resulting density functional:

$$\Omega(\{\rho(\mathbf{r})\},T,\mu;\{w(\mathbf{r})\},\{V(\mathbf{r})\})=\int d\mathbf{r}\, f_h(\rho(\mathbf{r}),T)+\tfrac{1}{2}\int d\mathbf{r}\int d\mathbf{r}'\tilde{w}(|\mathbf{r}-\mathbf{r}'|)\rho(\mathbf{r})\rho(\mathbf{r}') -\mu\int d\mathbf{r}\,\rho(\mathbf{r})+\int d\mathbf{r}\,\rho(\mathbf{r})V(\mathbf{r})\ . \tag{2.2}$$

The first term on the right-hand side of Eq. (2.2) represents the free energy of the reference system of particles interacting via the short-range potential $w_h(r)$. This free energy is evaluated in the local approximation; $f_h(\rho,T)$ is the free energy density of a uniform reference system with number density ρ. The second term includes the effect of long-range interactions. This contribution is determined by $\tilde{w}(\mathbf{r})$ which for large r is identical to $w(r)$; for small r it is modified, and smoothed in a well-defined way [35]. The second term in Eq. (2.2) neglects correla-

tions between the fluid particles: the two-particle density $\rho^{(2)}(\mathbf{r},\mathbf{r}')$ is replaced by the product of two one-particle densities $\rho(\mathbf{r})\rho(\mathbf{r}')$. This is equivalent to replacing the two-particle distribution function $g^{(2)}$ by its large-distance limit $g^{(2)}=1$. Actually, it turns out that in the analysis presented below one can use without additional complications instead of Eq. (2.2), a more sophisticated version of the density functional,

$$\Omega_{\mathrm{ld}}(\{\rho(\mathbf{r})\},T,\mu;\{w(\mathbf{r})\},\{V(\mathbf{r})\})=\int d\mathbf{r}\, f_h(\rho(\mathbf{r}),T) + \frac{k_BT}{2}\int d\mathbf{r}\int d\mathbf{r}'\rho(\mathbf{r})\rho(\mathbf{r}')e^{-\beta w_h(|\mathbf{r}-\mathbf{r}'|)}[1-e^{-\beta w_l(|\mathbf{r}-\mathbf{r}'|)}] -\mu\int d\mathbf{r}\,\rho(\mathbf{r})+\int d\mathbf{r}\,\rho(\mathbf{r})V(\mathbf{r}) , \tag{2.3}$$

which results from replacing the two-particle distribution function by its low-density limit (for details, see Refs. [36,37]).

All the results obtained for the simple version, Eq. (2.2), can be straightforwardly translated into those following from Eq. (2.3) by replacing the spherically symmetric potential $\tilde{w}(r)$ by

$$\tilde{g}(r)=k_BTe^{-\beta w_h(r)}[1-e^{-\beta w_l(r)}] , \tag{2.4}$$

which is also spherically symmetric. For reasons of simplicity in the following we employ the version given in Eq. (2.2) and at the end we shall also discuss the results which correspond to the more accurate expression given in Eq. (2.3). The third term on the right-hand side of Eq. (2.2) is characteristic for the grand canonical functional while the last term accounts for the possible interaction of the fluid particles with an external potential including gravity.

As far as the particle-particle interactions are concerned we are particularly interested in the case of long-range van der Waals interactions decaying at large distances as $\tilde{w}(r)\sim r^{-6}$. Since, however, our analysis does not require the specification of the actual type of interactions the final formulas can be evaluated for arbitrary spherically symmetric interaction potentials $\tilde{w}(r)$.

III. THE EFFECTIVE INTERFACE HAMILTONIAN

Below we derive the expression for the effective interface Hamiltonian, i.e., the cost in free energy required to deform the initially flat liquid-vapor interface into a rippled configuration. Thus the concept of the effective interface Hamiltonian as used in this paper has a broader meaning than is frequently attributed to it in the literature [6,8–10,15] because it is not restricted to describe only the cost in free energy due to the increase of the interfacial area.

In order to perform this analysis systematically we enclose the coexisting liquid and vapor into the parallelepiped with extensions $2L_x$, $2L_y$, and $2L_z$ along the x, y, and z axis, respectively. This will allow us to separate the bulk, surface, line, and point contributions to the grand canonical density functional and eventually to find the contribution identified as the effective interface Hamiltonian. Since in this finite-size system the coexisting liquid and vapor are surrounded by vacuum, there appear additional interfaces, such as the liquid-vacuum and the vapor-vacuum interfaces. They have to be identified and must be separated from the expression to be analyzed. According to the description given in the Introduction we evaluate the functional in Eq. (2.2) for the density configuration $\hat{\rho}(\mathbf{r})=\rho_{\mathrm{int}}(z-f(\mathbf{R}),T)$ where $z=f(\mathbf{R})$, $\mathbf{R}=(x,y)$, describes the mean position of the liquid-vapor interfaces. In our analysis we disregard bubbles and overhangs because the thermodynamic state of the system is assumed to be far away from the critical point. The splitting of the free energy functional into the different types of contributions mentioned above will be performed for the specific sharp-kink model of the intrinsic density profile which we adopt in this paper. The actual intrinsic profile varies smoothly across the interface from the bulk liquid density ρ_l on one side to the bulk va-

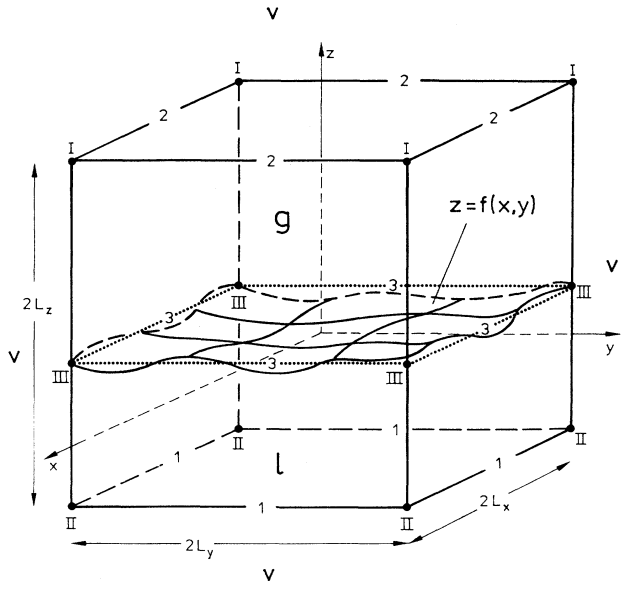

FIG. 1. The coexisting liquid (l) and vapor (g) phases are enclosed in a box $-L_x\le x\le L_x$, $-L_y\le y\le L_y$, $-L_z\le z\le L_z$ and surrounded by vacuum (v). The local position of the liquid-vapor interface is denoted by $f(x,y)$. The symbols 1 and 2 refer to the line tensions τ_{vvl} and τ_{vvg}, respectively [Eqs. (3.14) and (3.15)], whereas the symbol 3 refers to the line tension τ_{lvg} [Eq. (3.16)] corresponding to the case $f(x,y)=0$ (dotted line). The symbols I, II, and III refer to the appropriate point tensions $\eta_{(7v)g}$, $\eta_{7(v)l}$, and $\eta_{(3v)g(3v)l}$, respectively; $\eta_{(3v)g(3v)l}$ corresponds to the case $f(x,y)=0$ [Eqs. (3.18)–(3.20)].

por density ρ_g on the other side. The width of the interfacial region is of the order of the bulk correlation length ξ which itself is of the order of the molecular diameter provided the system is not too close to its critical state [38]. In order to be able to proceed analytically we replace this intrinsic density profile by its sharp-kink approximation

$$\bar{\rho}_{\rm int}(z)=\rho_g(T)\Theta(z)+\rho_l(T)\Theta(-z)\ , \tag{3.1}$$

where $\Theta(z)$ denotes the Heaviside function; the piecewise constant density changes discontinuously from ρ_l to ρ_g at the interface (see Fig. 1). The sharp-kink approximation to the intrinsic density profile has been successfully employed in the microscopic analysis of the wetting transitions [2]. It is known to lead to results, for example, for the effective interface potential, which reflect the essential features of the wetting transitions and on the other hand are obtainable without the computational complications which one encounters when one is dealing with the smooth variation of the intrinsic density profile [39,40]. After inserting the sharp-kink density profile [Eq. (3.1)] into Eq. (2.2), which is tantamount to evaluating the grand canonical density functional under the constraint of a fixed interface location specified by the function $f(x,y)$, one obtains for large system sizes the following expression for the grand canonical functional Ω in which the bulk (Ω^b), surface (Ω^s), line (Ω^l), and point (Ω^p) contributions are isolated:

$$\Omega=\Omega^b+\Omega^s+\Omega^l+\Omega^p+\Delta\Omega\ ; \tag{3.2}$$

$\Delta\Omega$ denotes the remaining terms. The explicit forms of Ω^l, Ω^p, and $\Delta\Omega$ depend on the asymptotic behavior of the shape of the interface $f(x,y)$ for $|x|,|y|\to\infty$. By assuming $f(x,y)\sim R^{-(1+\delta)}$ for $R=(x^2+y^2)^{1/2}\to\infty$ and $\delta>0$ one obtains after some algebra the following expressions:

$$\Omega^b=4L_xL_yL_z[\omega_b(\rho_l,T,\mu)+\omega_b(\rho_g,T,\mu)]\ , \tag{3.3}$$

$$\Omega^s=4L_xL_y\sigma_{lg}^{\rm int}+4L_xL_y(\sigma_{vl}+\sigma_{vg})+4(L_x+L_y)L_z(\sigma_{vl}+\sigma_{vg})\ , \tag{3.4}$$

$$\Omega^l=4(L_x+L_y+L_z)(\tau_{vvvl}+\tau_{vvvg})+4(L_x+L_y)\tau_{lvvg}\ , \tag{3.5}$$

$$\Omega^p=4\eta_{(7v)g}+4\eta_{(7v)l}+4\eta_{(3v)g(3v)l}-\tfrac{1}{2}(\rho_l-\rho_g)^2\int_{-\infty}^{+\infty}dx\int_{-\infty}^{+\infty}dy\int_{-\infty}^{+\infty}dx'\int_{-\infty}^{+\infty}dy'\int_0^{\infty}dz\int_0^{f(x',y')-f(x,y)}dz'\bar{w}(|\mathbf{r}'-\mathbf{r}|)\ , \tag{3.6}$$

and

$$\Delta\Omega(L_x,L_y,L_z)\to 0\ \text{ for } L_x,L_y,L_z\to\infty\ ; \tag{3.7}$$

for finite-size effects in interfacial tensions see Ref. [41].

In Eqs. (3.3)–(3.7) we have used the following notation:

$$\omega_b(\rho,T,\mu)\equiv f_h(\rho,T)+\tfrac{1}{2}w_0\rho^2-\mu\rho \tag{3.8}$$

is the (mean-field) grand canonical free energy density where

$$w_0=\int d\mathbf{r}\,\bar{w}(r)\ , \tag{3.9}$$

$$\sigma_{vl}=-\tfrac{1}{2}\rho_l^2\int_0^{\infty}dx\,t(x)\ , \tag{3.10}$$

$$\sigma_{vg}=-\tfrac{1}{2}\rho_g^2\int_0^{\infty}dx\,t(x)\ , \tag{3.11}$$

and

$$\sigma_{lg}^{\rm int}=-\tfrac{1}{2}(\rho_l-\rho_g)^2\int_0^{\infty}dx\,t(x) \tag{3.12}$$

denote the liquid-vacuum, vapor-vacuum, and liquid-vapor surface tension, respectively, and

$$t(z)=\int_z^{\infty}dz'\int_{-\infty}^{+\infty}dx'\times\int_{-\infty}^{+\infty}dy'\bar{w}[r'=(x'^2+y'^2+z'^2)^{1/2}]. \tag{3.13}$$

Analogously,

$$\tau_{vvvl}=\tfrac{1}{2}\rho_l^2\int_0^{\infty}dx\int_0^{\infty}dy\,t(x,y)\ , \tag{3.14}$$

$$\tau_{vvvg}=\tfrac{1}{2}\rho_g^2\int_0^{\infty}dx\int_0^{\infty}dy\,t(x,y)\ , \tag{3.15}$$

and

$$\tau_{lvvg}=\tfrac{1}{2}(\rho_l-\rho_g)^2\int_0^{\infty}dx\int_0^{\infty}dy\,t(x,y) \tag{3.16}$$

represent the line tensions denoted in Fig. 1 by 1, 2, and 3, respectively, with

$$t(x,y)=\int_x^{\infty}dx'\int_y^{\infty}dy'\int_{-\infty}^{+\infty}dz'\bar{w}(r')\ , \tag{3.17}$$

$$\eta_{(7v)g}=-\tfrac{1}{2}\rho_g^2\int_0^{\infty}dx\int_0^{\infty}dy\int_0^{\infty}dz\,t(x,y,z)\ , \tag{3.18}$$

$$\eta_{(7v)l}=-\tfrac{1}{2}\rho_l^2\int_0^{\infty}dx\int_0^{\infty}dy\int_0^{\infty}dz\,t(x,y,z)\ , \tag{3.19}$$

and

$$\eta_{(3v)g(3v)l}=-\tfrac{1}{2}(\rho_l-\rho_g)^2\times\int_0^{\infty}dx\int_0^{\infty}dy\int_0^{\infty}dz\,t(x,y,z)\ , \tag{3.20}$$

represent the point tensions denoted in Fig. 1 by I, II, and III, respectively, with

$$t(x,y,z)=\int_x^{\infty}dx'\int_y^{\infty}dy'\int_z^{\infty}dz'\bar{w}(r')\ . \tag{3.21}$$

Some of the terms present in Eqs. (3.4)–(3.6) are easily identified as the artificial ones mentioned above which result from the finite size of the system. These include all the terms in Eq. (3.4) except the first one which is the contribution to the free energy from the *flat* vapor-liquid

interface which is proportional to the intrinsic liquid-vapor surface tension $\sigma_{lg}^{\rm int}$, all the terms in Eq. (3.5), and the first three terms in Eq. (3.6); see Fig. 1. Accordingly, the capillary wave Hamiltonian $\mathcal{H}(\{f\})$ is given by the fourth term in Eq. (3.6), which is a nonlocal and nonbilinear functional of the interface configuration $f(x,y)$:

$$\mathcal{H}(\{f\})=\int_{\mathbb{R}^2} d^2R\, h_0(\mathbf{R},\{f\}) , \tag{3.22a}$$

with

$$h_0(\mathbf{R},\{f\})=-\tfrac{1}{2}(\rho_l-\rho_g)^2\int_{\mathbb{R}^2} d^2R'\int_0^\infty dz\int_0^{f(\mathbf{R}')-f(\mathbf{R})} dz'\,\tilde{w}(|\mathbf{r}'-\mathbf{r}|) . \tag{3.22b}$$

If the system is exposed to gravity [i.e., $V(z)=mGz$, where m is the mass of the particles] the effective interface Hamiltonian in Eq. (3.22) contains an extra term which is equal to $(m/2)(\rho_l-\rho_g)G\int dx\int dy\, f^2(x,y)$.

Before discussing the relation between the effective interface Hamiltonian as described by Eq. (3.22) and the standard phenomenological expressions for this Hamiltonian (see below) we point at two obvious features of Eq. (3.22): (i) $\mathcal{H}(\{f+\text{const}\})=\mathcal{H}(\{f\})$ and (ii) $\mathcal{H}(\{f=\text{const}\})=0$.

The first property means that in an infinite system of coexisting liquid and vapor the cost in free energy for shifting the interface uniformly by an arbitrary distance is zero. The second property means that the extra cost in free energy described by the effective interface Hamiltonian is zero for a flat interface. These two properties are also displayed by the standard phenomenological effective interface Hamiltonian [6,8–10,15]

$$\mathcal{H}^{(s)}(\{f\})=\bar{\sigma}_{lg}\int dx\int dy\{[1+(\nabla f)^2]^{1/2}-1\} , \tag{3.23}$$

where $\bar{\sigma}_{lg}$ is a phenomenological parameter identified as the liquid-vapor surface tension.

The relation between $\mathcal{H}(\{f\})$ and $\mathcal{H}^{(s)}(\{f\})$ can be established by observing that due to the decay of the integrand $\tilde{w}(|\mathbf{r}-\mathbf{r}'|)$ for large $|\mathbf{r}-\mathbf{r}'|$ the main contribution to the integral in Eq. (3.22) comes from those regions where $\mathbf{R}=(x,y)$ and $\mathbf{R}'=(x',y')$ are close to each other. On the other hand, the interface described by $f(x,y)$ is smooth because it includes only fluctuations with wavelengths larger than the bulk correlation length ξ. Accordingly, the upper limit of the z' integration in Eq. (3.22), i.e., $f(x',y')-f(x,y)$, is small for the dominant contributions. It is straightforward to show (see Appendix A) that Eq. (3.23) follows from Eq. (3.22) by expanding the difference $f(x',y')-f(x,y)$ in powers of $x'-x$ and $y'-y$,

$$\begin{aligned} f(x',y')-f(x,y)=&f_x(x'-x)+f_y(y'-y)\\ &+\tfrac{1}{2}f_{xx}(x'-x)^2+f_{xy}(x'-x)(y'-y)\\ &+\tfrac{1}{2}f_{yy}(y'-y)^2+\cdots , \end{aligned} \tag{3.24}$$

and by keeping only the linear terms. In this approximation Eq. (3.22) reduces to Eq. (3.23) with the surface tension coefficient $\bar{\sigma}_{lg}$ given by $\sigma_{lg}^{\rm int}$ in Eq. (3.12). In the next step also the second-order terms, i.e., those including the derivatives f_{xx}, f_{xy}, and f_{yy} are taken into account upon inserting the expansion in Eq. (3.24) into Eq. (3.22). In this case the effective interface Hamiltonian reduces to the expression which in addition to the standard contribution [see Eq. (3.23)] due to the change of the interfacial area contains terms describing the curvature corrections to this standard contribution. Locally the shape of the interface as described by the function $f(x,y)$ is given by the mean curvature $H(x,y)$

$$H=\frac{f_{xx}(1+f_y^2)+f_{yy}(1+f_x^2)-2f_{xy}f_xf_y}{2(1+f_x^2+f_y^2)^{3/2}} , \tag{3.25}$$

and the Gaussian curvature $K(x,y)$

$$K=\frac{f_{xx}f_{yy}-f_{xy}^2}{(1+f_x^2+f_y^2)^2} . \tag{3.26}$$

The derivation of the curvature terms is much more lengthy and cumbersome than the derivation of the standard term given in Appendix A. Therefore we do not document these details which go beyond the limits of any reasonable presentation. Instead in Appendix B we quote only the main points. As the result of this tedious calculation one obtains rigorously up to terms quadratic in f_{xx}, f_{xy}, and f_{yy} the following form of the effective interface Hamiltonian which resembles the Helfrich Hamiltonian [20,21]:

$$\begin{aligned} \mathcal{H}(\{f\})=&\sigma_{lg}^{\rm int}\int dx\int dy\{[1+(\nabla f)^2]^{1/2}-1\}\\ &+\kappa\int dx\int dy[1+(\nabla f)^2]^{1/2}[H^2-\tfrac{1}{3}K]+\cdots , \end{aligned} \tag{3.27}$$

where

$$\kappa=-\tfrac{9}{8}(\Delta\rho)^2\int_0^\infty dz\, z^2t(z)=-\frac{3\pi}{16}(\Delta\rho)^2\int_0^\infty dr\, r^5\tilde{w}(r) \tag{3.28}$$

and

$$\sigma_{lg}^{\rm int}=-\tfrac{1}{2}(\Delta\rho)^2\int_0^\infty dz\, t(z)=-\frac{\pi}{2}(\Delta\rho)^2\int_0^\infty dr\, r^3\tilde{w}(r) . \tag{3.29}$$

Both the coefficient $\sigma_{lg}^{\rm int}$ in the standard part of the effective interface Hamiltonian and κ in front of the curvature terms are proportional to moments of the long-range attractive part of the interparticle potential $\tilde{w}(r)$ and are thus positive [see Eqs. (3.12), (A3), (A6), (3.28), and (3.29)]. This positivity of the coefficients holds also for the more sophisticated version of the density-functional theory given in Eq. (2.3). Also the integrands in both terms on the right-hand side of Eq. (3.27) are non-negative. The non-negativity of the integrand in the

first term is obvious. The non-negativity of the integrand in the second term is easy to check by using the representation of the mean and Gaussian curvatures in terms of the principal curvatures k_1 and k_2 [42]; $H=\frac{1}{2}(k_1+k_2)$ and $K=k_1k_2$. One obtains $H^2-\frac{1}{3}K=\frac{1}{12}(k_1+k_2)^2+\frac{1}{6}(k_1^2+k_2^2)\geq 0$. Thus each of the first two terms in the gradient expansion shares with the full nonlocal effective interface Hamiltonian given in Eq. (3.22) the non-negativity property (see Appendix C).

At this point it is worthwhile to compare the form of our effective interface Hamiltonian, Eq. (3.27), with those obtained by other authors. In fact the combination of the curvature terms as it appears in Eq. (3.27), i.e., $H^2-\frac{1}{3}K$, is the same as in Ref. [26] and it is proportional to the bending energy of a thin elastic plate. On the other hand, the expression derived in Ref. [22] in the limit $\xi\to 0$, which corresponds to our case [see Eq. (4.6) in Ref. [22]], is proportional to $H^2+\frac{1}{3}K$ and thus leads to a difference in sign. This last expression for the bending energy leads to an effective interface Hamiltonian *density* h_0 which is not positive definite for arbitrary interfacial configuration. However, we would like to note that for interface configurations we are concerned with, i.e., interfaces which are not closed, without bubbles, and with $f(R\to\infty)=0$, one has $\int_{\mathbb{R}^2} d^2R\, K(x,y)=0$ so that the Gaussian curvature gives a vanishing contribution to $\mathcal{H}$.

For long-range forces the interparticle potential $\tilde{w}(r)$ decays as $\tilde{w}(r\to\infty)=Ar^{-(d+\tau)}$ where d is the spatial dimension. For nonretarded van der Waals forces $\tau=3$ and the coefficient κ is infinite. If, however, retardation is taken into account, i.e., $\tau=4$, κ remains finite but it depends sensitively on the distance at which the crossover towards retardation sets in. Nonetheless in this case as for any power-law decay the higher moments of $\tilde{w}(r)$ diverge and so the gradient expansion, which contains higher-order derivatives of f, breaks down for long-range interactions.

In the case of exponentially decaying forces the individual terms in Eq. (3.27) exist but their sum diverges. Only interparticle potentials with a *finite support* guarantee the convergence of the gradient expansion (see Appendix D). These properties remain valid also in the case when the potential $\tilde{w}(r)$ is replaced by the low-density limit of the two-particle distribution function corresponding to Eq. (2.4). The above-mentioned divergence problems have their counterpart in the field-theoretic derivation of the effective interface Hamiltonian. There the coefficients of the gradient expansion in Eq. (3.27) are proportional to the moments of the square of the derivative of the intrinsic profile: $\int_{-\infty}^{\infty} dz\, z^n(d\rho_{\rm int}/dz)^2$. This result has been derived for contactlike interactions for which $\rho_{\rm int}(z)$ approaches its bulk values exponentially. If, however, within this approach one adopts the decay law of the intrinsic profile as that of the so-called van der Waals tails which are induced by the long-range interparticle forces, one has $\rho_{\rm int}(|z|\to\infty)\sim|z|^{-\tau}$ and the coefficients in the gradient expansion become infinite for $n\geq 2\tau+1$.

For a general intrinsic profile the expansion in Eq. (3.27) contains also a term linear in H which, together with the term quadratic in H, gives rise to the spontaneous curvature [17–22]. However, the coefficient of this term linear in H vanishes if $\rho_{\rm int}(z)$ is antisymmetric around $z=0$. This is in accordance with our result, because the sharp-kink profile which we use for $\rho_{\rm int}$ [see Eq. (3.1)] is antisymmetric.

IV. WAVE-VECTOR-DEPENDENT SURFACE TENSION AND SCATTERING EXPERIMENTS

In order to elucidate the relevance of the nonlocal character of the effective interface Hamiltonian given in Eq. (3.22) and in order to obtain further insight into its analytic structure we study it in Fourier space. With $\tilde{f}(\mathbf{q})=\int_{\mathbb{R}^{d-1}} d^{d-1}R\, e^{-i\mathbf{q}\cdot\mathbf{R}}f(\mathbf{R})$, where $\mathbf{R}=(x,y)$ in $d=3$, one finds

$$\mathcal{H}(\{f\})=\tfrac{1}{2}\int\frac{d^{d-1}q}{(2\pi)^{d-1}}q^2\sigma(q)|\tilde{f}(\mathbf{q})|^2+O(\tilde{f}^3)\ . \tag{4.1}$$

The wave-vector-dependent surface tension

$$\sigma(q)=(\rho_l-\rho_g)^2\frac{v(q)-v(0)}{q^2} \tag{4.2}$$

is determined by an appropriate Fourier transform

$$v(q)=\int_{\mathbb{R}^{d-1}} d^{d-1}R\, e^{-i\mathbf{q}\cdot\mathbf{R}}\tilde{w}(\mathbf{r}=(\mathbf{R},0)) \tag{4.3}$$

of the interaction potential. According to our previous remarks the q integration in Eq. (4.1) is confined to $|\mathbf{q}|\leq q_{\max}$ with $q_{\max}=\xi^{-1}$. The form of Eq. (4.1) has already been discussed previously in the literature [11,41,43]. There it is postulated by first transforming the quadratic approximation to Eq. (3.23) into Fourier space,

$$\tilde{\mathcal{H}}(\{f\})=\tfrac{1}{2}\bar{\sigma}_{lg}\int\frac{d^{d-1}q}{(2\pi)^{d-1}}q^2|\tilde{f}(\mathbf{q})|^2\ , \tag{4.4}$$

and then by generalizing it phenomenologically into the nonlocal form of Eq. (4.1) by introducing the q-dependent surface tension in which configurations with short wavelengths renormalize the surface tension for long wavelengths [11,43]. Within our approach Eq. (4.1) is a consequence of Eq. (3.22) after truncating contributions which are of higher order than quadratic (the so-called non-Gaussian contributions). It turns out that based on Eq. (3.1) the q-dependent surface tension [see Eq. (4.2)] is determined by the Fourier transform of the interparticle potential. One can easily check that $\sigma(q=0)=\sigma_{lg}^{\rm int}$ which means that in the limit of long wavelengths the quadratic contributions to the standard and to the nonlocal effective interface Hamiltonian are identical [44]. But due to the long-range character of the interparticle potential [i.e., $\tilde{w}(r\to\infty)=Ar^{-(d+\tau)}$] the correction $\sigma(q)-\sigma(q=0)$ to the leading term contains both analytic contributions $\sim q^{2k}$, $k=1,2,\ldots$, and nonanalytic ones. The leading nonanalytic term is given by

$$[\sigma(q\to 0)-\sigma(q=0)]_{\text{nonanalytic}}=A\pi^{(d+1)/2}2^{-(\tau+1)}\left[\sin\left[\pi\frac{\tau+3}{2}\right]\Gamma\left[\frac{\tau+d}{d}\right]\Gamma\left[\frac{\tau+3}{2}\right]\right]^{-1}q^{\tau-1} \tag{4.5}$$

for $\tau\neq 2k+1$; Γ denotes the gamma function. For $\tau\to 2k+1$ this term retains its nonanalytic character because in this limit the prefactor in Eq. (4.5) diverges and leads via a resonance with the analytic term $\sim q^{2k}$ to a logarithmic singularity. This is actually the case for the nonretarded van der Waals forces with $\tau=3$. For $d=3$ and the model potential $\bar{w}(r)=A(a^2+r^2)^{-3}$ where A is negative and where a is proportional to the particle diameter one obtains

$$\sigma(q)=\sigma_{lg}^{\text{int}}\left[1-\left[\frac{aq}{2}\right]^2[-\ln(aq)+\ln 2+\tfrac{3}{4}-C]+O(q^4\ln q)\right]; \tag{4.6}$$

$C\simeq 0.577\,215$ is Euler's constant. The above nonanalyticities for long-range forces in Fourier space reflect the breakdown of the gradient expansion which amounts to a series expansion in powers of q^2. Equation (4.6) shows that $\sigma(q)$ exhibits at least a local *maximum* at $q=0$. This property is not tied to the nonanalytic contribution from long-range forces. For interaction potentials with $\tau>4$ one finds

$$\begin{aligned}\sigma(q)&=\tfrac{1}{4}(\rho_l-\rho_g)^2|\bar{w}_2|(1-\tfrac{1}{16}q^2|\bar{w}_4/\bar{w}_2|+\cdots)\\&=\sigma_{lg}^{\text{int}}(1-\tfrac{1}{6}q^2\kappa/\sigma_{lg}^{\text{int}}+\cdots),\end{aligned} \tag{4.7}$$

where $\bar{w}_j=\int_{\mathbb{R}^2}d^2R\,R^j\bar{w}(\mathbf{r}=(\mathbf{R},0))$, so that $\sigma(q)$ reaches its value at $q=0$ from *below*.

It is instructive to compare the wave-vector-dependent surface tension $\sigma(q)$ in Eq. (4.7) as obtained from the *nonlocal* effective interface Hamiltonian with the corresponding quantity $\tilde{\sigma}(q)$, defined as in Eq. (4.1), which would follow from the *local* Hamiltonian in Eq. (3.27) after truncation of all nonbilinear terms:

$$\tilde{\sigma}(q)=\sigma_{lg}^{\text{int}}(1+\tfrac{1}{2}q^2\kappa/\sigma_{lg}^{\text{int}}+\cdots). \tag{4.8}$$

As can be seen by inspection $\tilde{\sigma}(q)$ reaches its value at $q=0$, which is the same as for $\sigma(q)$, from *above*, i.e., one has $\sigma(q)\neq\tilde{\sigma}(q)$. The reason for this difference is that Eq. (3.27) contains terms which are proportional to fourth-order derivatives and to products of third-order and first-order derivatives; these terms contribute to the term $\sim q^2$ in $\sigma(q)$ but they are not captured by the curvature terms H^2 and K. However, $\sigma(q)$ does contain these contributions. Thus the Helfrich Hamiltonian [Eq. (3.27)] does not allow one to infer the correct wave-vector-dependent surface tension even in the limit $q\to 0$. In fact, the wave-vector-dependent surface tension $\tilde{\sigma}(q)$, which corresponds to the Helfrich Hamiltonian, exhibits the wrong qualitative behavior compared with that obtained from the correct expression, i.e., $\sigma(q)$. It is important to note that all previous studies in the literature [16–19,22–26] have finally led to the Helfrich Hamiltonian and thus missed the difference between $\sigma(q)$ and $\tilde{\sigma}(q)$. Thus even if the range of the interactions would be sufficiently short in order to allow for the existence of the gradient expansion (see Appendix D), the Helfrich Hamiltonian would be inadequate for describing the experimentally relevant quantities (see below) which depend on $\sigma(q)$.

As outlined in the Introduction $e^{-\beta\mathcal{H}(\{f\})}$ serves as the statistical weight for determining thermal averages which involve fluctuations on length scales larger than ξ. *Inter alia,* such averages determine the actual shape of the interface which can be probed by reflectivity and ellipsometry experiments [38,45–51]. These measurements allow one to determine the moments

$$F_i^2=\int_0^{q_m}dq\,q^{d-2+i}\langle|\tilde{f}(\mathbf{q})|^2\rangle, \tag{4.9}$$

with $i=0$ and 1 corresponding to reflectivity and ellipsometry experiments, respectively. $q_m=2\pi/\lambda_{\min}$ denotes the aforementioned momentum cutoff inherent in the capillary wave picture. We take $\lambda_{\min}=\xi$. If ξ is defined as the second moment of the two-point correlation function $G(r=|\mathbf{r}_1-\mathbf{r}_2|)=\langle\rho(\mathbf{r}_1)\rho(\mathbf{r}_2)\rangle-\langle\rho(\mathbf{r}_1)\rangle\langle\rho(\mathbf{r}_2)\rangle$ one has $\xi^2=(1/2d)[\int d^dr\,r^2G(r)]/\int d^dr\,G(r)$. For the density-functional approach given in Eq. (2.2) one finds $\xi^2=|w_2|[2d(w_0+\partial^2f_h/\partial\rho^2)]^{-1}$, where $\partial^2f_h/\partial\rho^2$ is evaluated at the equilibrium bulk densities at coexistence and where $w_j=\int d^dr\,r^j\bar{w}(r)$. For $T\to T_c$, ξ diverges as $\xi_-=\xi_0^{(-)}(1-T/T_c)^{-\nu}$, $\nu=\frac{1}{2}$, with $\xi_0^{(-)}=[(1/4d)|w_2/w_0|]^{1/2}$. Explicit calculations based on Eq. (2.2) show that far below T_c (and this is the temperature range we are focusing on [see Eq. (3.1)]) ξ_0^- happens to be a reasonable approximation for $\xi(T\ll T_c)$. Since $\xi_0^-=3a$ we obtain for our model potential $\lambda_{\min}=3a$ so that $aq_m=2\pi/3$. This cutoff is of the order of the inverse molecular diameter in accordance with experimental estimates [38]. Within the nonlocal Gaussian approximation of the effective interface Hamiltonian [see Eq. (4.1)] one obtains in the presence of gravity

$$\langle|\tilde{f}(\mathbf{q})|^2\rangle_G=\frac{k_BT}{mG\Delta\rho+\sigma(q)q^2}. \tag{4.10}$$

By inserting the expression for the q-dependent surface tension [see Eq. (4.2)], the moments F_i^2 given in Eq. (4.9) can be evaluated. It is important to note that the moments remain cutoff dependent. In order to make contact with the full capillary wave Hamiltonian as described by Eq. (3.22) [for which the average $\langle|\tilde{f}(\mathbf{q})|^2\rangle$ cannot be calculated analytically due to its non-Gaussian character] and with other approaches we write the thermal average of $|\tilde{f}(\mathbf{q})|^2$ in a form analogous to Eq. (4.10):

$$\langle|\tilde{f}(\mathbf{q})|^2\rangle=\frac{k_BT}{mG\Delta\rho+\sigma_{lg}^{\text{int}}q^2\Sigma(q)}. \tag{4.11}$$

The function $\Sigma(q)$ defined in Eq. (4.11) consists of the Gaussian term $\Sigma_G(q)=\sigma(q)/\sigma_{lg}^{\text{int}}$ and the remaining con-

tributions $\Sigma_{nG}(q)$ due to the non-Gaussian fluctuations: $\Sigma(q)=\Sigma_G(q)+\Sigma_{nG}(q)$. For the *local* Gaussian approximation, which corresponds to Eq. (4.4), one has $\sigma(q)=\sigma_{lg}^{int}$ so that $\Sigma_G^l(q)=1$. In order to estimate $\Sigma_{nG}(q)$ we employ a saddle-point-like approximation. To this end we evaluate the effective interface Hamiltonian given in Eq. (3.22) for a sinusoidal capillary wave profile $f(x,y)$ [by using our model potential $\bar{w}(r)=A(a^2+r^2)^{-3}$], normalize it properly, and after subtracting from it the Gaussian contributions we consider the rest $\hat{\Sigma}_{nG}(q)$ as a mean-field-like approximation to $\Sigma_{nG}(q)$. We parametrize the capillary wave by $f_\Lambda(\mathbf{R},q)=f_0 e^{-|x|/\Lambda}\sin qx$ in the limit $\Lambda\to\infty$ which is translationally invariant in the y direction [32]. In the spirit of the saddle-point approximation we choose f_0 to be the mean amplitude. Since at low temperatures and in the presence of gravity the mean thickness of the interface is of the order of the molecular diameter we take $f_0=a$ [38]. The properly normalized effective interface Hamiltonian $\mathcal{H}(\{f_\Lambda(\mathbf{R},q)\})$ is denoted by $F(q)$,

$$F(q)=\lim_{\Lambda\to\infty}\left\{\frac{4\mathcal{H}(\{f_\Lambda(\mathbf{R},q)\})}{q^2\sigma_{lg}^{int}f_0^2L_y\Lambda}\right\}, \tag{4.12}$$

so that [52]

$$\hat{\Sigma}_{nG}(q)=F(q)-\Sigma_G(q)\ . \tag{4.13}$$

Our results are displayed in Fig. 2 where $F(q)$ is evaluated for the full effective interface Hamiltonian [see Eq. (3.22), full line], for the Gaussian nonlocal model [see Eq. (4.1), dashed line], for the non-Gaussian local model [see Eq. (3.23), dash-dotted line], and for the Gaussian local model [see Eq. (4.4), dotted line]. As expected for $q\to 0$ all approximations agree with the full nonlocal $\mathcal{H}$. For larger q they differ so that close to q_m the difference between the standard local Gaussian expression (dotted line) and the full nonlocal expression (full line) reaches 60%.

Now the question arises of how the above findings depend on temperature. Within the density-functional theory approach of Eq. (2.2) and for the sharp-kink approximation [Eq. (3.1)] the temperature dependence of the effective interface Hamiltonian enters only via the density difference $\rho_l-\rho_g$ [see Eq. (3.22b)] and can be factored out [see Eqs. (3.29) and (4.12)]. We expect these expressions to be reliable at low temperatures just above the triple point T_t. The density-functional theory given by Eqs. (2.3) and (2.4) allows us, however, to infer at least certain aspects of the actual temperature dependence of

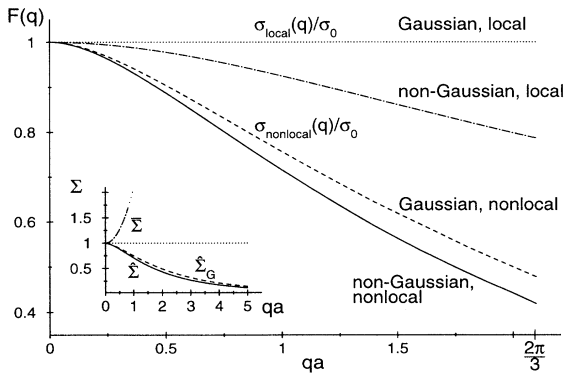

FIG. 2. $F(q)=\lim_{\Lambda\to\infty}[4\mathcal{H}(\{f_\Lambda(\mathbf{R},q)\})/(q^2\sigma_{lg}^{int}f_0^2L_y\Lambda)]$, where L_y is the lateral system size in y direction. The full, dash-dotted, and dotted curves correspond to $\mathcal{H}$ evaluated for h_0 given by Eq. (3.22b), Eq. (3.23) with $\bar{\sigma}_{lg}=\sigma_{lg}^{int}$ [see Eq. (3.29)], and $h_0=\frac{1}{2}\sigma_{lg}^{int}(\nabla f)^2$, respectively. The dashed curve corresponds to Eq. (4.1). Due to the above normalization the dashed curve is identical to $\sigma(q)/\sigma_{lg}^{int}$. The inset compares $\hat{\Sigma}(q)=F(q)$, which has a turning point at $aq_t=0.79$ with $\bar{\Sigma}(q)$ for $T/T_c=0.7$ and $a^3\Delta\rho=0.69$. $\hat{\Sigma}_G=\sigma_{nonlocal}(q)/\sigma_0=F(q)$ if in Eq. (4.12) $\mathcal{H}$ has the form given by Eq. (4.1). $\bar{\Sigma}$ is defined in the main text [see Eq. (4.15)].

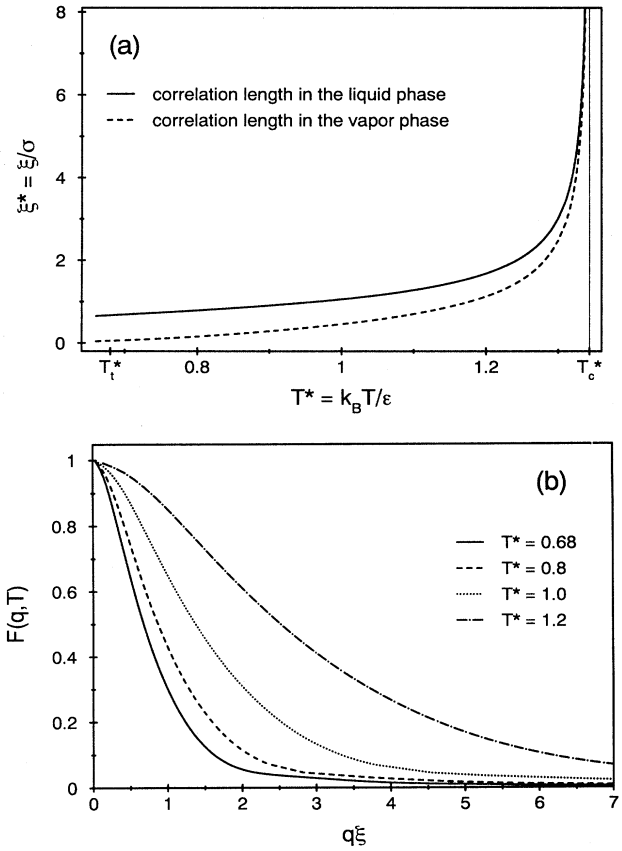

FIG. 3. (a) The correlation lengths of the coexisting liquid (l) and vapor (g) phases plotted as function of the dimensionless temperature $T^*=k_BT/\varepsilon$ as obtained from Eq. (2.3) for a Lennard-Jones interaction potential parametrized by ε and σ (see the main text). The triple point temperature is given by $T_t^*\simeq 0.68$ and the critical temperature by $T_c^*\simeq 1.3430$ [37]. (b) $F(q,T)$ is the generalized wave-vector-dependent surface tension as defined in Eq. (4.12) for $f_0=\sigma$. $\mathcal{H}$ is given by Eq. (3.22) with $\bar{w}(r)$ replaced by $\bar{g}(r)$ [see Eq. (2.4)]; $\bar{g}(r)$ is evaluated for a Lennard-Jones potential (see Ref. [37]). $\xi=(\xi_l+\xi_g)/2$ is taken from (a) for various temperatures T^*. Our choice for the wave-vector cutoff is $q_m\xi=2\pi$. The standard capillary wave model predicts $F(q,T)=F_s(q)\equiv 1$.

the effective interface Hamiltonian. These results must be discussed cautiously because they are still based on the sharp-kink approximation [Eq. (3.1)]. Therefore they can be used only as long as the correlation length is still rather small so that the intrinsic density profile still varies sharply at the interface. Figure 3(a) displays the correlation length (as defined above) in the liquid (ξ_l) and in vapor (ξ_g) phases at coexistence as obtained from the density-functional theory given by Eq. (2.3). These curves correspond to a Lennard-Jones interaction potential $w(r)=4\varepsilon[(\sigma/r)^{12}-(\sigma/r)^6]$ which differs from our above model potential. (For details concerning the relation between w_h, w_l, and w and the corresponding bulk phase diagram see Ref. [37].) Since in our context the correlation length plays the role of measuring the thickness of the intrinsic density profile, in the following we take $\xi=(\xi_l+\xi_g)/2$. (In the discussion of the temperature dependence of the effective interface Hamiltonian in the literature this significant difference between ξ_l and ξ_g has so far been ignored [12,22–25]. Therefore all quantitative conclusions drawn there which depend on ξ must be considered with reservation.) In Fig. 3(b) we show the function $F(q,T)$ for various reduced temperatures $T^*=k_BT/\varepsilon$ as function of $q\xi$ with ξ taken from Fig. 3(a) for each temperature. Note that $T_t^*\simeq 0.68$ and $T_c^*\simeq 1.3430$ [37]. The function $F(q,T)$ has been obtained numerically according to Eq. (4.12) for $f_0=\sigma$ and $\mathcal{H}$ given by Eq. (3.22) with $\bar{w}(r)$ replaced by $\bar{g}(r)$ [see Eq. (2.4) and Ref. [37]]. As before one has $F(q=0,T)=1$ and $F(q\to\infty,T)\sim q^{-2}$. As discussed above, the wave-vector cutoff $q_{\max}$ is given approximately by $\lambda_{\min}=\xi$, i.e., $q_{\max}\xi=2\pi$ with ξ taken from Fig. 3(a). The general trend in Fig. 3(a) is that $F(q,T)$ increases as function of the temperature for a given value of $q\xi(T)$. This means that for high temperatures the difference between the standard local and Gaussian theory (compare Fig. 2), i.e., $F_s(q)=1$ and the actual wave-vector-dependent surface tension $F(q,T)$ decreases. Within our low-temperature approximation we cannot answer the question whether $F(q,T\to T_c)$ as function of $q\xi$ will approach a curve which differs from F_s. However, from the analysis of Blokhuis and Bedeaux (BB) [22] one can infer that there may be a nontrivial limiting function for $T\to T_c$. Based on the Helfrich Hamiltonian and their microscopic expressions for $\sigma_{lg}^{\rm int}$ and κ (recall that the term $\sim K$ vanishes in our case) their result can be cast into the form [note the qualitatively different q dependence compared with Fig. 3(b)]

$$\tilde{\sigma}_{\rm BB}(q\to 0,T\to T_c)/\sigma_{lg}^{\rm int}=1+\left[\frac{\pi^2}{6}+2\right](q\xi_{\rm BB})^2+\cdots , \tag{4.14}$$

which must be compared with $F(q,T)$ and $F_s(q)=1$ (see also Fig. 2). (The definition of the correlation length by Blokhuis and Bedeaux differs from ours; however, close to T_c this difference amounts only to a different prefactor of the power law $\xi(T\to T_c)=\xi_0^-[(T_c-T)/T_c]^{-\nu}$.) Thus at least for the function $\tilde{\sigma}(q)$ one obtains a "universal" nontrivial form for $T\to T_c$. The question whether this is also true for the experimentally relevant function $\sigma(q)$ [$\neq\tilde{\sigma}(q)$, see Eqs. (4.7) and (4.8)], in particular in the presence of long-range forces [see Eq. (4.6)], must be addressed by an improved analysis which goes beyond our present sharp-kink approximation [Eq. (3.1)]. Finally it is also instructive to display the function $E(q,T)=F(q,T)(q\sigma)^2$ as function of q. (In the bilinear approximation one has $E_{\rm bil}(q,T)=(q\sigma)^2\sigma(q)/\sigma(0)$ [see Eq. (4.1)].) According to Eq. (4.12) $E(q,T)$ gives, up to constant factors, the cost in free energy in units of the intrinsic surface tension for maintaining a capillary wave with a given wavelength $\lambda=2\pi/q$. Figure 4 shows that this free energy vanishes for long wavelengths proportional to q^2 as predicted by the standard capillary wave model. However, we find it interesting that our microscopic approach predicts that this free energy reaches a maximum at $q_c\simeq 3/\sigma$ and approaches a finite value for large q. For high temperatures the position of this maximum shifts to smaller values of q. Although this structure of $E(q,T)$ occurs at the edge of the applicability of the effective interface model [$\lambda_c\simeq(2\pi/3)\sigma$] and although our temperature analysis is limited to low temperatures Fig. 4 leads us to speculate whether within a refined theory the position $q_c(T)$ may serve as a natural wave-vector cutoff q_m which is then no longer imposed externally by the somehow arbitrary requirement $q_m\xi=2\pi$ but follows from the effective interface Hamiltonian itself. If it was true this would solve a longstanding discussion in the literature.

At this stage it is worthwhile to make contact between our results and the phenomenological approach by Meunier [50]. In particular we are interested in comparing both the structure of the q-dependent surface tension and the cutoff dependence of the experimentally accessi-

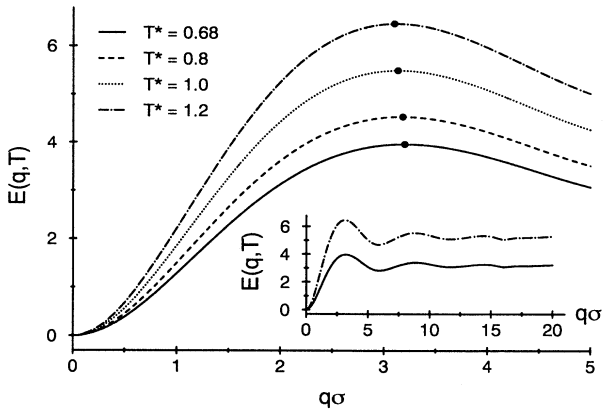

FIG. 4. $E(q,T)=(q\sigma)^2F(q,T)$ with $F(q,T)$ taken from Fig. 3 represents the cost in free energy in units of the intrinsic surface tension for maintaining a capillary wave with a given wavelength $2\pi/q$ [Eq. (4.12)]; σ denotes one of the Lennard-Jones interaction parameters. $E(q,T)$ reaches a maximum (denoted by full circles) at $q_c(T)$ which shifts to lower values for higher temperatures. For small q, $E(q,T)$ vanishes $\sim q^2$ whereas it approaches a finite value at large q (see the inset). In the bilinear approximation, which is not used here, $E(q,T)$ would be given by the wave-vector-dependent surface tension: $E_{\rm bil}(q,T)=(q\sigma)^2\sigma(q,T)/\sigma_{lg}^{\rm int}$.

ble moments F_i^2 [see Eq. (4.9)]. Meunier's approach is based on a mode-coupling theory applied to the local Hamiltonian

$$\overline{\mathcal{H}}(\{f\})=\tfrac{1}{2}\sigma_{lg}\int dx \int dy[(\nabla f)^2-\tfrac{1}{4}(\nabla f)^4] . \quad (4.15)$$

$\overline{\mathcal{H}}$ retains the first two terms of the expansion of $[1+(\nabla f)^2]^{1/2}-1$. One should note that $\overline{\mathcal{H}}$ violates the positivity requirement and favors configurations with large spatial variations. Equation (4.13) leads to [50] $\overline{\Sigma}_G=1$ and $\overline{\Sigma}^l_{\rm nG}(q\to 0)=(3k_BT/8\pi)q^2/\sigma_{lg}^{\rm int}$ which is positive [as is the case for $\bar{\sigma}(q)$ in Eq. (4.8)].

Meunier's line of argument is to extrapolate the small q behavior of $\overline{\Sigma}(q)$ to large q so that $q^2\overline{\Sigma}(q\to\infty)\sim q^4$. According to Eqs. (4.9) and (4.11) this assumption leads to a decay of the integrand for the moments F_i^2 [see Eq. (4.9)] $\sim q^{d-6+i}$. Thus for $d=3$ and $i\le 1$ the moments F_i^2 would remain finite even if the momentum cutoff q_m is shifted to infinity. This reasoning would therefore lead to the conclusion that for the experimentally observable quantities F_i^2 the momentum cutoff is irrelevant.

However, our results show that $q^2\Sigma^{nl}(q\to\infty)=$const and therefore the integrand of the moments F_i^2 varies as q^{d-2+1} for large q [see Eq. (4.9)]. Thus we conclude that the moments F_i^2 are strongly cutoff dependent. Figure 2 and its inset demonstrate the qualitative difference between Meunier's result $\overline{\Sigma}(q)$ and our estimate $\hat{\Sigma}(q)$. Even if our saddle-point-like approximation for the non-Gaussian contribution to Σ would turn out to need improvements, we expect in any case that the *leading* term of $\Sigma_{\rm nG}(q\to 0)$ is analytic in q^2. This means that in the limit of small q the logarithmic singularity in $\Sigma_G(q)$, which we have determined exactly, will dominate the non-Gaussian contribution [see Eq. (4.6)]. Therefore the nonlocal character of the Hamiltonian should always lead to a *decreasing* function $\Sigma(q)$, at least for small q.

We conclude that the current interpretation of reflectivity and ellipsometry data for fluid interfaces requires reconsiderations due to the importance of the long-range van der Waals forces, which lead to an inherent nonlocal description of the fluctuations. This analysis should be accompanied by an improved estimate of the non-Gaussian contributions which goes beyond our saddle-point-like approximation as well as by a description of the intrinsic interface profile which goes beyond the sharp-kink approximation.

V. SUMMARY

Starting from the microscopic density-functional theory for an inhomogeneous simple fluid [Eqs. (2.2) and (2.3)], which consists of the coexisting liquid and vapor phases far from the critical point, and by systematically separating bulk, surface, line, and point contributions to this density functional we derive the expression for the effective interface Hamiltonian [Eq. (3.22)]. It is a *nonlocal* and a *nonbilinear* functional of the interface configuration and thus differs from all effective interface Hamiltonians used so far in the literature which have always been *local* functionals of the interface configuration. We have shown that this effective interface Hamiltonian is positive definite for arbitrary interface configuration (Appendix C). In the limit of slowly varying interfaces it reduces to the standard effective interface Hamiltonian which, except for the cost in free energy due to the increase of the interface area caused by capillary waves, contains also terms proportional to the mean curvature squared and to the Gaussian curvature [Eq. (3.27)]. We have derived microscopic expressions for the coefficients multiplying these terms [Eqs. (3.28) and (3.29)]. They are proportional to the moments of the interparticle potential or of the two-particle distribution function [Eq. (2.4)]. Thus, e.g., for van der Waals interaction potentials decaying at large distances like r^{-6} the intrinsic surface tension is finite but the coefficient in front of the curvature terms is infinite. This divergence of the curvature coefficient reflects the breakdown of the gradient expansion for any interaction potential which decays like a power law. This aspect becomes more transparent by transforming the capillary wave Hamiltonian into Fourier space and by keeping only terms quadratic in the interface configurations [Eq. (4.1)]. This allows one to retain nonlocality within the Gaussian approximation. The nonlocality is reflected by the wave-vector dependence of the surface tension which is proportional to an appropriate Fourier transform of the interparticle potential [Eq. (4.2)]. For long-range forces, the wave-vector-dependent surface tension turns out to be a *nonanalytic* function for small wave vectors [Eqs. (4.5) and (4.6)]. This nonanalyticity reflects the divergence of the coefficients in the gradient expansion in real space. Furthermore we find that the gradient expansion fails even for exponentially decaying interaction potentials. It is only valid if these potentials have a strictly finite support (Appendix D). For a certain model potential we compare our nonlocal and nonbilinear effective interface Hamiltonian quantitatively with various approximations thereof, in particular with those used in the literature so far (Fig. 2). We find qualitative differences. In particular, the interpretation of scattering data from fluid interfaces in terms of the capillary wave picture is cutoff dependent, contrary to previous claims in the literature [Eq. (4.9)]. It turns out that the Helfrich Hamiltonian [Eq. (3.27)] leads to a qualitatively wrong wave-vector dependence of the surface tension [Eqs. (4.7) and (4.8)] even in that case in which the gradient expansion exists. The difference between the predictions of the standard capillary wave theory [Eq. (3.23)] and of the nonlocal and nonbilinear effective interface Hamiltonian [Eq. (3.22)] become smaller for high temperatures but persist to be significant (Fig. 3). There are indications that the nonlocal effective interface Hamiltonian suggests a natural intrinsic wave-vector cutoff which is not imposed externally (Fig. 4).

ACKNOWLEDGMENTS

We thank G. Flöter, T. Getta, and W. Koch for numerical assistance leading to Figs. 1–4 and R. Bausch, J. Sengers, and H. Wagner for helpful discussions. One of the authors (M.N.) acknowledges the support by a grant of the Committee for Scientific Research in Poland.

APPENDIX A: DERIVATION OF THE STANDARD EFFECTIVE INTERFACE HAMILTONIAN

In order to derive the standard effective interface Hamiltonian $\mathcal{H}^{(s)}(\{f\})$ [see Eq. (3.23)] from the nonlocal expression $\mathcal{H}(\{f\})$ [see Eq. (3.22b)] we replace the upper limit of the z' integration by $f_x(x,y)(x'-x)+f_y(x,y)(y'-y)$ and change the integration variables from (x,y,z,x',y',z') to $(x,y,z,x'-x,y'-y,z')$:

$$h_0(\mathbf{R},\{f\})=-\tfrac{1}{2}(\rho_l-\rho_g)^2\int_{\mathbb{R}^2}d^2R'\int_0^\infty dz\int_0^{x'f_x+y'f_y}dz'\tilde{w}(x',y',z'-z)\ . \tag{A1}$$

The integrand $\tilde{w}(x,y,z)$ in Eq. (A1) is a spherically symmetric function. Therefore it has the form

$$\tilde{w}(x,y,z)=p(x^2+y^2+z^2)\ , \tag{A2}$$

where $p(u)$ is a smooth function which vanishes for $u\to\infty$. The integration over the variables $\mathbf{R}'=(x',y')$ in Eq. (A1) is performed in polar coordinates $[\rho=(x'^2+y'^2)^{1/2},\varphi=\arctan(y'/x')]$ so that

$$h_0(\mathbf{R},\{f\})=-\tfrac{1}{2}(\rho_l-\rho_g)^2\int_0^{2\pi}d\varphi\int_0^\infty d\rho\,\rho\int_0^\infty dz\int_0^{\rho\alpha(\varphi)}dz'p(\rho^2+(z'-z)^2)\ , \tag{A3}$$

where the function

$$\alpha(\varphi)=f_x\cos\varphi+f_y\sin\varphi \tag{A4}$$

depends parametrically (via f_x and f_y) on $\mathbf{R}=(x,y)$. After integrations by parts and changes of variables one obtains the following expression:

$$h_0(\mathbf{R},f)=-\tfrac{1}{2}(\rho_l-\rho_g)^2\int_0^{2\pi}d\varphi\,\alpha(\varphi)\arctan[\alpha(\varphi)]\times\int_0^\infty dR\,R^3p(R^2)\ . \tag{A5}$$

From Eqs. (3.13) and (A3) a straightforward calculation leads to

$$\int_0^\infty dR\,R^3p(R^2)=\frac{1}{\pi}\int_0^\infty dz\,t(z)\ . \tag{A6}$$

On the other hand, one has

$$\int_0^{2\pi}d\varphi\,\alpha(\varphi)\arctan[\alpha(\varphi)]=2\pi[(1+f_x^2+f_y^2)^{1/2}-1]\ . \tag{A7}$$

After combining Eqs. (A5)–(A7) one obtains the standard expression for the effective interface Hamiltonian given in Eq. (3.23) with $\bar{\sigma}_{lg}=\sigma_{lg}^{\rm int}$ [see Eq. (3.12)].

APPENDIX B: CURVATURE TERMS

After inserting the expansion in Eq. (3.24) into Eq. (3.22b) one obtains with $\delta f(x',y',x,y)=x'f_x+y'f_y+\frac{1}{2}(x'f_{xx}+2x'y'f_{xy}+y'^2f_{yy})$:

$$h_0(\{f\})=-\tfrac{1}{2}(\Delta\rho)^2\int_{-\infty}^{+\infty}dx'\int_{-\infty}^{+\infty}dy'\int_0^\infty dz\int_0^{\delta f(x',y',x,y)}dz'\tilde{w}(x',y',z'-z)\ . \tag{B1}$$

In the next step the right-hand side of Eq. (B1) is expanded in powers of the second-order derivatives f_{xx}, f_{xy}, and f_{yy} and only terms up to second order in these derivatives are kept. The coefficients in front of these terms depend also parametrically on the first-order derivatives f_x and f_y; as far as *this* dependence is concerned no further expansion is made. For a spherically symmetric potential $\tilde{w}(x,y,z)$ it is convenient to perform the integrations over x' and y' in Eq. (B1) by using polar coordinates. The prefactors of the terms linear in f_{xx}, f_{xy}, and f_{yy} vanish due to this spherical symmetry. After a tedious calculation—which includes no further approximations—the dependence of the prefactors of the terms quadratic in f_{xx}, f_{xy}, and f_{yy} with respect to the interparticle potential can be cast into a simple integral form while their dependence on f_x and f_y is summed up leading to the following final form:

contributions to $h_0(f)$ bilinear in f_{xx} , f_{xy} , and f_{yy}

$$=\left[-\frac{3\pi}{16}(\Delta\rho)^2\int_0^\infty dr\,r^5\tilde{w}(r)\right](1+f_x^2+f_y^2)^{1/2}[H^2-\tfrac{1}{3}K]\ . \tag{B2}$$

The mean (H) and the Gaussian (K) curvature are given by Eqs. (3.25) and (3.26).

APPENDIX C: NON-NEGATIVITY OF THE EFFECTIVE INTERFACE HAMILTONIAN

In order to prove the non-negativity of the nonlocal capillary wave Hamiltonian given in Eq. (3.22) we rewrite it in the following way after integrating by parts:

$$\mathcal{H}(\{f\})=-\tfrac{1}{2}(\Delta\rho)^2\int_{-\infty}^{+\infty}dx\int_{-\infty}^{+\infty}dx'\int_{-\infty}^{+\infty}dy\int_{-\infty}^{+\infty}dy'\int_0^{\infty}dz\int_0^{\Delta f}dz'\,\tilde{w}(x'-x,y'-y,z'-z)$$
$$=-\tfrac{1}{2}(\Delta\rho)^2\int_{-\infty}^{+\infty}dx\int_{-\infty}^{+\infty}dx'\int_{-\infty}^{+\infty}dy\int_{-\infty}^{+\infty}dy'\left\{\Delta f\int_{-\Delta f}^{\infty}dz\,\tilde{w}(x'-x,y'-y,z)\right.$$
$$\left.+\int_0^{\infty}dz\int_0^{\Delta f}dz'\,z'\frac{d}{dz}\tilde{w}(x'-x,y'-y,z'-z)\right\}, \quad \text{(C1)}$$

where we have used the abbreviation $\Delta f\equiv f(x',y')-f(x,y)$. Using the spherical symmetry of the potential $\tilde{w}(x,y,z)$ the above expression can be written as

$$\mathcal{H}(\{f\})=-\tfrac{1}{2}(\Delta\rho)^2\int_{-\infty}^{+\infty}dx\int_{-\infty}^{+\infty}dx'\int_{-\infty}^{+\infty}dy\int_{-\infty}^{+\infty}dy'\left[\int_0^{\Delta f}dz(\Delta f-z)\tilde{w}(x'-x,y'-y,z)\right]. \quad \text{(C2)}$$

Since the potential $\tilde{w}$ is negative (recall the difference between w and $\tilde{w}$ [see Eq. (2.2)]) it is easy to see that independent of the sign of Δf the integrand in Eq. (C2) is non-positive which proves the non-negativity of the effective interface Hamiltonian.

APPENDIX D: CONVERGENCE OF THE GRADIENT EXPANSION

In order to analyze the convergence of the gradient expansion of the effective interface Hamiltonian [Eq. (3.22)] for simplicity we consider the case that the interfacial profile $f(\mathbf{R})$ is translationally invariant in the y direction and thus depends only on the variable x: $f(\mathbf{R})=\psi(x)$. In this case the analog of Eq. (3.22) has the form

$$\hat{\mathcal{H}}_{cw}(\{\psi\})=\int_{-\infty}^{\infty}dx\,\hat{h}_0(x,\{\psi\}), \quad \text{(D1)}$$

where

$$\hat{h}_0(x,\{\psi\})=-\tfrac{1}{2}(\Delta\rho)^2\int_{-\infty}^{\infty}dx'\int_0^{\infty}dz\int_0^{\psi(x')-\psi(x)}dz'\,\hat{w}(x'-x,z'-z) \quad \text{(D2)}$$

and

$$\hat{w}(x,z)=\int_{-\infty}^{\infty}dy\,\tilde{w}(x,y,z). \quad \text{(D3)}$$

After performing the gradient expansion along the lines described in Sec. III for a spherically symmetric interaction potential $\hat{w}(x,z)$,

$$\hat{w}(x,z)=\hat{p}(x^2+z^2), \quad \text{(D4)}$$

and by *analyzing exclusively those terms which contain only the second derivative of* ψ, i.e., $\psi''(x)$, one obtains as the result of tedious algebra the following series in powers of $\psi''(x)$:

$$\hat{h}_0(x,\{\psi\})=-\tfrac{1}{2}(\Delta\rho)^2\left\{\frac{\psi''(x)}{2}\int_{-\infty}^{+\infty}dx'\int_0^{\infty}dz\,\hat{w}(x',z)x'^2\right.$$
$$\left.+\sum_{n=2}^{\infty}(-1)^n\left[\frac{\psi''(x)}{2}\right]^n\frac{1}{n!}\int_{-\infty}^{+\infty}dx'x'^{2n}\hat{w}_{(n-2)}(x',0)\right\}, \quad \text{(D5)}$$

where $\hat{w}_{(k)}(x',0)\equiv(d^k/dz^k)\hat{w}(x',z)|_{z=0}$. By using the properties

$$\hat{w}_{(2k+1)}(x,0)=0,$$
$$\hat{w}_{(2k)}(x,0)=\frac{(2k)!}{k!}\frac{d^k}{d(x^2)^k}\hat{p}(x^2), \quad \text{(D6)}$$

and after integrating by parts Eq. (D5) can be cast into the following form:

$$\hat{h}_0(x,\{\psi\})=-\tfrac{1}{2}(\Delta\rho)^2\left\{\frac{\psi''(x)}{2}\int_{-\infty}^{+\infty}dx'\int_0^{\infty}dz\,\hat{w}(x',z)x'^2\right.$$
$$\left.+\sum_{k=1}^{\infty}(-1)^{k-1}\left[\frac{\psi''(x)}{2}\right]^{2k}\frac{2k+1}{2k-1}\frac{(4k)!}{2^{4k}}\frac{1}{(k!)^2}\frac{1}{(2k)!}\int_0^{\infty}dx\,x^{2k}t(x)\right\}, \quad \text{(D7)}$$

with the function $t(x)$ defined in Eq. (3.13) [see also Eq. (3.12)]. For interaction potentials decaying $\sim r^{(d+\tau)}$ the coefficients $\int_0^\infty dx\, x^{2k} t(x)$ of the terms $(\psi'')^{2k}$ are infinite for $k \geq (\tau-1)/2$. Thus we conclude that the gradient expansion fails for *any* power-law interaction. In order to test for *short-range forces* the absolute convergence criterion for the series in Eq. (D7), which in the present case takes the form

$$[\psi''(x)]^2 < \lim_{k\to\infty} \frac{\left| \int_0^\infty dx\, x^{2k} t(x) \right|}{\left| \int_0^\infty dx\, x^{2k+2} t(x) \right|} , \tag{D8}$$

we employ the following simple model potential:

$$t(x) = Be^{-\alpha x} . \tag{D9}$$

It is straightforward to check that in this case the condition in Eq. (D8) reduces to

$$[\psi''(x)]^2 < \lim_{k\to\infty} \frac{\alpha^2}{4k^2} = 0 . \tag{D10}$$

Since Eq. (D10) is violated for any nontrivial interface configuration we conclude that the gradient expansion breaks down even for exponentially decaying forces. It is noteworthy that one obtains similar results for the model potential $t(x) = B' e^{-\alpha' x^2}$. Finally for a model potential $t(x)$ which has a finite support,

$$t(x) = \begin{cases} t_0 & \text{for } 0 \leq x < \sigma \\ 0 & \text{elsewhere} , \end{cases} \tag{D11}$$

the criterion in Eq. (D8) reduces to

$$|\psi''(x)| < \frac{1}{\sigma} . \tag{D12}$$

Equation (D12) states that the gradient expansion is valid for all configurations which vary on a length scale larger than the range of the interaction potential. Therefore we find that the gradient expansion is only valid for interaction potentials between the fluid particles which have a strictly finite support.

[1] *Fluid Interfacial Phenomena,* edited by C. A. Croxton (Wiley, Chichester, 1986).

[2] S. Dietrich, in *Phase Transitions and Critical Phenomena,* edited by C. Domb and J. L. Lebowitz (Academic, London, 1988), Vol. 12, p. 1.

[3] *Liquids at Interfaces,* Les Houches Summer School Lectures, Session XLVIII, edited by J. Chavrolin, J. F. Joanny, and J. Zinn-Justin (Elsevier, Amsterdam, 1990).

[4] J. S. Rowlinson and B. Widom, *Molecular Theory of Capillarity* (Clarendon, Oxford, 1982).

[5] *Capillarity Today,* edited by G. Pétré and A. Sanfeld (Springer, Berlin, 1991).

[6] F. P. Buff, R. A. Lovett, and F. H. Stillinger, Phys. Rev. Lett. **15**, 621 (1965).

[7] J. D. van der Waals, Z. Phys. Chem. **13**, 657 (1984); for an English translation see J. S. Rowlinson, J. Stat. Phys. **20**, 197 (1979).

[8] B. Widom, in *Liquids, Freezing and Glass Transition,* Les Houches Lectures, Session LI, edited by J. P. Hansen, D. Levesque, and J. Zinn-Justin (Elsevier, Amsterdam, 1991).

[9] D. Jasnow, Rep. Prog. Phys. **47**, 1059 (1984).

[10] D. A. Huse, W. van Saarloos, and J. D. Weeks, Phys. Rev. B **32**, 233 (1985).

[11] J. M. J. van Leeuwen and J. V. Sengers, Physica A **157**, 839 (1989).

[12] J. V. Sengers and J. M. J. van Leeuwen, Phys. Rev. A **39**, 6346 (1989).

[13] J. D. Weeks, J. Chem. Phys. **67**, 3106 (1977).

[14] D. Bedeaux and J. D. Weeks, J. Chem. Phys. **82**, 972 (1985).

[15] H. W. Diehl, D. M. Kroll, and H. Wagner, Z. Phys. B **36**, 329 (1980).

[16] S. C. Liu and M. J. Lowe, J. Phys. A **16**, 347 (1983).

[17] M. P. A. Fisher and M. Wortis, Phys. Rev. B **29**, 6252 (1984).

[18] R. K. R. Zia, Nucl. Phys. **B251** [FS13], 676 (1985).

[19] G. Gompper and S. Zschocke, Europhys. Lett. **18**, 731 (1991); Phys. Rev. A **46**, 4836 (1992).

[20] W. Helfrich, Z. Naturforsch, Teil C **28**, 693 (1973).

[21] F. David, in *Statistical Mechanics of Membranes and Surfaces,* edited by D. Nelson, T. Piran, and S. Weinberg (World Scientific, Singapore, 1989).

[22] E. M. Blokhuis and D. Bedeaux, J. Chem. Phys. **95**, 6986 (1991); Physica A **184**, 42 (1992).

[23] V. Romero-Rochiń, C. Varea, and A. Robledo, Physica A **184**, 367 (1992).

[24] V. Romero-Rochiń, C. Varea, and A. Robledo, Phys. Rev. A **44**, 8417 (1991).

[25] V. Romero-Rochiń, C. Varea, and A. Robledo, in *Lectures on Thermodynamics and Statistical Mechanics,* edited by M. L. de Haro and C. Varea (World Scientific, Singapore, 1991), p. 10.

[26] J. B. Keller and G. J. Merchant, J. Stat. Phys. **63**, 1039 (1991).

[27] R. Evans, Adv. Phys. **28**, 143 (1979).

[28] R. Evans, in *Liquids at Interfaces,* Les Houches Lectures, Session XLVIII, edited by J. Chavrolin, J. F. Joanny, and J. Zinn-Justin (Elsevier, Amsterdam, 1990), p. 1.

[29] A. J. M. Yang, P. D. Fleming III, and J. H. Gibbs, J. Chem. Phys. **64**, 3732 (1976).

[30] J. H. Pérez-López and J. E. Puig, Physica A **172**, 309 (1991).

[31] A. Robledo, C. Varea, and V. Romero-Rochiń, Physica A **177**, 474 (1991).

[32] S. Dietrich and M. Napiórkowski, Physica A **177**, 437 (1991).

[33] M. Napiórkowski and S. Dietrich, Z. Phys. B **89**, 263 (1992).

[34] N. G. van Kampen, Phys. Rev. **135**, A362 (1964).

[35] J. Barker and D. Henderson, Rev. Mod. Phys. **48**, 587 (1976).

[36] P. I. Teixeira and M. M. Telo da Gamma, J. Phys. C **3**, 111 (1991).

[37] P. Frodl and S. Dietrich, Phys. Rev. A **45**, 7330 (1992).

[38] P. S. Pershan, Faraday Discuss. Chem. Soc. **89**, 231 (1990).

[39] S. Dietrich and M. Napiórkowski, Phys. Rev. A **43**, 1861 (1991).

[40] S. Dietrich, in *Phase Transitions in Surface Films 2,* Vol.

B267 of *NATO Advanced Study Institute, Series B: Physics*, edited by H. Taub, G. Torzo, H. Lauter, and S. C. Fain (Plenum, New York, 1991), p. 391.
[41] M. P. Gelfand and M. E. Fisher, Physica A **166**, 1 (1990).
[42] B. O'Neill, *Elementary Differential Geometry* (Academic, New York, 1966).
[43] R. F. Kayser, Phys. Rev. A **33**, 1948 (1986).
[44] D. M. Kroll, R. Lipowsky, and R. K. Zia, Phys. Rev. B. **32**, 1862 (1985).
[45] M. K. Sanyal, S. K. Sinha, K. G. Huang, and B. M. Ocks, Phys. Rev. Lett. **66**, 628 (1991).
[46] R. Braslau, M. Deutsch, P. S. Pershan, A. H. Weiss, J. Als-Nielsen, and J. Bohr, Phys. Rev. Lett. **54**, 114 (1985).
[47] J. S. Huang and W. W. Webb, J. Chem. Phys. **50**, 3677 (1969).
[48] E. S. Wu and W. W. Webb, Phys. Rev. A **8**, 2065 (1973).
[49] D. Beaglehole, Phys. Rev. Lett. **58**, 1434 (1987).
[50] J. Meunier, J. Phys. (Paris) **48**, 1819 (1987).
[51] D. Bonn and G. H. Wegdam, J. Phys. I (France) **2**, 1755 (1992).
[52] The expression analogous to Eq. (4.10) in Ref. [33] contains a misprint which places the factor 4 in the denominator instead of in the numerator as it should be.